Asian Journal of Chemistry; Vol. 29, No. 3 (2017), 475-479

ASIAN JOURNAL OF CHEMISTRY

https://doi.org/10.14233/ajchem.2017.20181

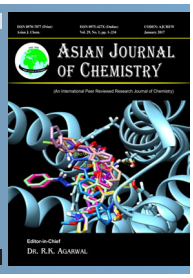

Fixed-Bed Adsorption of Metanil Yellow from Aqueous Solution on HNO_3-Treated-H_3PO_4-Activated Carbon from Gmelina Bark

BENIAH O. ISIUKU* and CALISTUS N. NWOSU

Department of Chemistry, Imo State University, Owerri, Nigeria

*Corresponding author: Tel: +234 8035731300; E-mail: obinnabisiuku@yahoo.com

Received: 11 July 2016; *Accepted*: 11 November 2016; *Published online*: 30 December 2016; AJC-18184

Fixed-bed adsorption studies were carried out to evaluate the efficiency of H_3PO_4-activated carbon treated with HNO_3 as an adsorbent for the removal of metanil yellow from aqueous solution under the effects of varying influent concentrations, bed heights and volumetric flow rates at solution pH 3 and at 29 °C. Experimental data were fitted into Thomas and Yoon-Nelson models. Increase in adsorption capacity with increase in initial concentration (except 100 mg/L), increase in bed height and decrease in flow rate was observed. Optimum equilibrium adsorption capacity 19.93 mg/g for influent concentration 50 mg/L, bed height 4.15 cm and flow rate 6 mL/min was obtained. The linear regression coefficients R^2 values of 0.6814 to 0.9627 for the Thomas and 0.7123 to 0.9664 for the Yoon-Nelson models showed both models fit in analyzing experimental data. The results show gmelina bark as a potential precursor for activated carbon production.

Keywords: Adsorption capacity, Carbon, Fixed-bed, Gmelina bark, Kinetic models, Metanil yellow.

INTRODUCTION

Dye wastewaters discharged from textile and dyestuff industries impact on water bodies generating growing public concern over their toxicity and carcinogenicity [1]. The persistent nature of reactive dyes complicates wastewater treatment within the textile industry. Removal of dyestuffs from wastewater occurs by either biological or physicochemical methods such as adsorption, oxidation-reduction, chemical coagulation, ozone treatment and membrane filtration [2].

Metanil yellow is an azo dye soluble in water and used in beverages production, leather, paper and textile industries. It is also used as a stain and an indicator in acid-base volumetric analysis [3]. Metanil yellow has detrimental health effects on humans [4].

Adsorption is a surface phenomenon where a substance binds to the surface of the other on an atomic or molecular scale [5]. Physical adsorption techniques are generally considered as the preferred means for removing and purifying organic substances due to their high efficiency and ability to separate a wide range of chemical compounds [6]. Adsorption in fixed-bed columns using activated column has been widely used in industrial processes for the removal of contaminants from aqueous textile industry effluents, since it does not require the addition of chemical compounds in the separation process [7]. The continuous adsorption in fixed-bed is often desired from industrial point of view. It is simple to be operated and can be scaled up from a laboratory process [8,9].

Activated carbon is the most commonly used adsorbent and has proved to be an effective material for the removal of various pollutants from wastewater. However, the activated carbon process is found to be an expensive treatment process, because of the high cost of activated carbon [10].

The aim of this study was to produce activated carbon from gmelina bark in order to reduce the cost of carbon-based adsorbents and also save the non-renewable natural resources and produce valuable product with potential applications in pollution control even in fixed-bed wastewater treatment.

EXPERIMENTAL

Adsorbate: Metanil yellow also named 3-(4-anilinophenylazo) benzene sulphonic acid sodium salt, C.I. Acid yellow 36, Tropaeoline G and Acid leather yellow R (Fig. 1) used in this work, a product of Merck, was purchased at Onitsha, Nigeria. The adsorbate was used without further treatment. The stock solution was prepared by dissolving 1 g per dm^3 solution in distilled water.

Preparation of activated carbon: The method of Ahmad and Hameed [8] was employed in this work. The gmelina bark collected from gmelina tree at Amakohia, Owerri, Nigeria, was washed with distilled water to remove dirt and dust. After

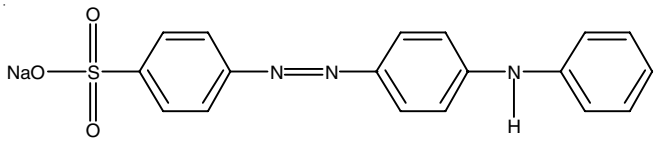

Fig. 1. Structure of metanil yellow

drying in sunlight for 3 days, the bark was ground into small particles. The biomass was soaked in 20 % H_3PO_4 at a ratio of 1 biomass: 3 acid by mass overnight. Excess acid was drained off and the biomass dried. The dry acid-treated bark was carbonized at 500 °C for 5 h, cooled and washed with distilled water to pH 6. The washed carbon was dried in a hot air oven at 110 °C for 2 h. After drying and cooling the carbon was treated with 1 M HNO_3 solution overnight. Excess acid was decanted off and the carbon was washed with distilled water to pH 6, dried at 110 °C, for 2 h, cooled and sieved to get 0.420-0.841 mm particle sizes. The carbon was packed in an airtight plastic container. A sample of the carbon was analyzed for the physicochemical properties.

Adsorption process: The adsorption column was a cylindrical Pyrex glass tube of measurement 30 cm in length and 1.8 cm internal diameter. The adsorption tube was plugged at the base with glass wool. Known masses of the carbon (equivalent to 2.1, 4.15 or 6.3 cm height) were introduced. The adsorbent was sealed with glass wool and the remaining space in the tube packed with glass beads. The glass beads ensured uniformity in the flow of the adsorbate. Different concentrations of the dye obtained by diluting the stock solution with distilled water (25, 50 or 100 mg/L) were made to flow upward through the column at specific flow rates (6, 17 or 26 mL/min) for a given time and 29 °C with the help of a metering pump (Chem-Tech Pal No. 0-111.808). Samples of the effluent were collected at specific intervals for analysis using a UV-visible spectrophotometer (Shimadzu UV-752, Japan) at λ_{max} 440nm.

Analysis of fixed-bed column data: The major characteristic of fixed-bed column adsorption is the history of effluent concentration [11]. These concentration – time curves are commonly called breakthrough curves and the time at which the effluent concentration reaches the threshold value is called the breakthrough time. The breakthrough curves show the loading behaviour of the adsorbate to be removed from solution in a fixed-bed column and is usually expressed in terms of adsorbed adsorbate concentration C_{ad}, influent adsorbate concentration C_o, effluent adsorbate concentration, C_t, or normalized concentration (C_t/C_o), as a function of time or volume of effluent for a given bed height or adsorbent mass [8,12-14].

Effluent volume (V_{eff}) can be calculated from eqn. 1:

$$V_{eff} = Qt_{tot} \quad (1)$$

where, Q and t_{tot} are the volumetric flow rate (mL/min) and the total flow time (min).

The area under the breakthrough curve (A) obtained by integrating the adsorbed concentration [C_{ad} (mg/L)] *versus* time (min) plot can be used to find the total adsorbed adsorbate quantity (maximum column capacity) (q_{tot}). For a given influent concentration and flow rate, q_{tot} is determined from eqn. 2:

$$q_{tot} = \frac{QA}{1000} = \frac{Q}{1000}\int_{t=o}^{t=t_{tot}} C_{ad}dt \quad (2)$$

The total amount of dye sent to the column (m_{tot}) is determined using eqn. 3:

$$m_{tot} = \frac{C_o Qt_{tot}}{1000} \quad (3)$$

Total removal (%) of adsorbate (column performance) with respect to flow volume can also be found from the ratio of total adsorbed quantity of adsorbate (q_{tot}) to the total amount of adsorbate sent to the column (m_{tot}) eqn. 4:

$$\text{Total removal } (\%) = \frac{100q_{tot}}{m_{tot}} \quad (4)$$

Equilibrium uptake of the adsorbate q_e or column adsorption capacity at the end of total flow time is defined by eqn. 5: as the maximum column capacity per amount of adsorbent used x(g):

$$q_e = \frac{q_{tot}}{x} \quad (5)$$

Un-adsorbed adsorbate concentration at equilibrium in the column, C_e(mg/L) can be calculated from eqn. 6:

$$C_e = \frac{(m_{tot} - q_{tot})1000}{V_{eff}} = \frac{(m_{tot} - q_{tot})100}{Q_{tot}} \quad (6)$$

Column adsorption modelling: A number of mathematical models have been developed for the evaluation of efficiency and applicability of the column models for large scale operations. They include the Adams-Bohart, Wolborska, Thomas, Clark, Yoon-Nelson and the Bed Depth Service Time (BDST) models. However, Thomas and Yoon-Nelson models were used to analyze the behaviour of adsorbent-adsorbate system in this work.

Thomas model: Thomas model is one of the most general and widely used models in column performance simulation. The expression by Thomas for an adsorption column [15,16] is given as eqn. 7:

$$\frac{C_t}{C_o} = \frac{1}{1 + \exp[K_{Th}(q_o x - C_o V_{eff})/Q]} \quad (7)$$

where, C_t (mg/L) is the effluent adsorbate concentration, C_o (mg/L) the influent adsorbate concentration, q_o (mg/g) the maximum adsorption capacity of the adsorbent, x(g) mass of adsorbent used, K_{Th} (mL/mg min) the Thomas rate constant and Q (mL/min) the volumetric flow rate.

The value t (min) is expressed as eqn. 8:

$$t = \frac{V_{eff}}{Q} \quad (8)$$

The linearized form of Thomas model is expressed as eqn. 9:

$$\ln\{[C_o/C_t] - 1\} = \frac{K_{Th}q_o 1000x}{Q} - K_{Th}C_o t \quad (9)$$

Thomas rate constant (or kinetic coefficient) K_{Th} and the maximum adsorbate adsorption capacity of the adsorbent q_o can be determined from the plot $\ln[(C_o/C_t) - 1]$ *versus* t.

Yoon-Nelson model: Yoon-Nelson model [17] is based on the assumption that the rate of decrease in the probability of adsorbate and the probability for a single component system is expressed as eqn. 10:

$$\ln\left[\frac{C_t}{(C_o - C_t)}\right] = K_{YN}t - \tau K_{YN} \quad (10)$$

where, C_t (mg/L) is the effluent concentration, C_o (mg/L) influent concentration, K_{YN} (min^{-1})

Yoon-Nelson rate constant, t (min) sampling time and τ (min) the time required for 50 % adsorbate breakthrough.

The calculation of theoretical breakthrough curves for a single-component system requires the determination of the parameters K_{YN} and τ for the adsorption from the slope and intercept, respectively of a straight-line plot of ln $[C_t/(C_o - C_t)]$ *versus* sampling time t.

The slope yields K_{YN} and the intercept - τK_{YN}. Based on the obtained value of τ, the adsorption capacity, q_{oYN} can be calculated [12] applying eqn. 11:

$$q_{oYN} = \frac{q_{tot}}{x} = \frac{C_o Q \tau}{1000x} \quad (11)$$

RESULTS AND DISCUSSION

Effect of influent concentration: Various influent dye solution concentrations (25, 50 and 100 mg/L) were used for the adsorption at pH 3, bed height 4.15 cm, flow rate 6 mL/min and temperature 29 °C. The breakthrough curves shown in Fig. 2 show that breakthrough could not be achieved within 360 min for influent concentration of 25 mg/L. The breakthrough time for 50 mg/L was 240 min while for 100 mg/L the breakthrough time was 90 min showing that breakthrough time decreased with increase in influent concentration. The inverse relationship between influent concentration and breakthrough time as well as saturation time was as a result of lower mass-transfer flux from the bulk solution to the adsorbent surface due to weaker driving force at lower concentrations [11,18,19].

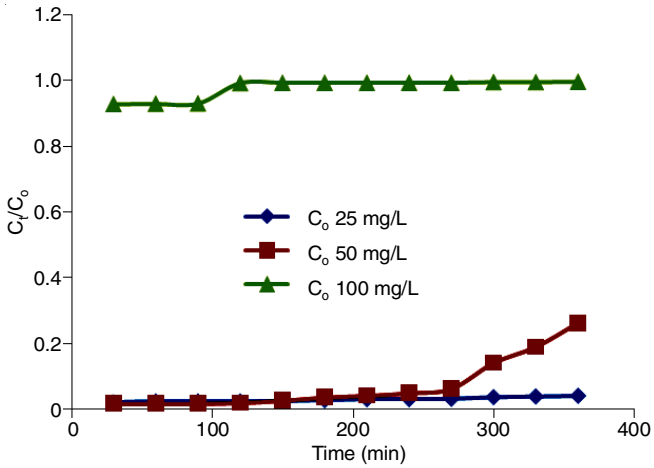

Fig. 2. Effect of influent concentration on the fixed-bed adsorption of metanil yellow on HNO_3-treated-H_3PO_4-activated carbon from gmelina bark

High sorbate concentration easily saturates the column bed, thereby decreasing the breakthrough time. Table-1 shows the adsorption capacity to increase from 12.96 to 19.93 mg/g as influent concentration increased from 25 to 50 mg/L.

TABLE-1
ADSORPTION DATA FOR FIXED BED CARBON COLUMN FOR METANIL YELLOW ADSORPTION AT DIFFERENT PROCESS PARAMETERS

Influent conc. (mg/L)	Carbon bed height (cm)	Flow rate (mL/min)	q_{tot} (mg/g)	q_e (mg/g)	Total removal (%)
25	4.15	6.0	51.84	12.96	96.00
50	4.15	6.0	79.72	19.93	73.81
100	4.15	6.0	0.88	0.22	0.41
25	2.10	6.0	6.32	1.58	11.70
25	6.30	6.0	28.40	7.10	52.59
25	4.15	17.0	12.56	3.14	8.21
25	4.15	24.0	4.44	1.11	2.06

However, there was decrease from 19.93 to 0.22 mg/g in adsorption capacity as influent concentration increased from 50 to 100 mg/L. This trend was observed in literature [20-22]. The reason for the drastic decrease in adsorption capacity when influent concentration was 100 mg/L might be as a result of generation of species which competed with the dye ions for binding sites on the adsorbent [20].

Effect of adsorbent bed height: Breakthrough curves for the adsorption of metanil yellow on gmelina bark carbon in a fixed bed at the influent concentration of 25 mg/L, flow rate of 6 mL/min and different bed heights are shown in Fig. 3. Results show that the lower the bed height, the faster the saturation except for 4.15 cm bed height where breakthrough could not be reached within 360 min. Table-1 shows that the equilibrium adsorption capacity increased with increase in adsorbent bed height. This is supported by the work of Salman *et al*. [23]. However the optimum bed height in this work was 4.15 cm. The increase in adsorption with bed height was due to the increase in adsorbent doses in higher beds which provided greater adsorption sites for the dye ions [17].

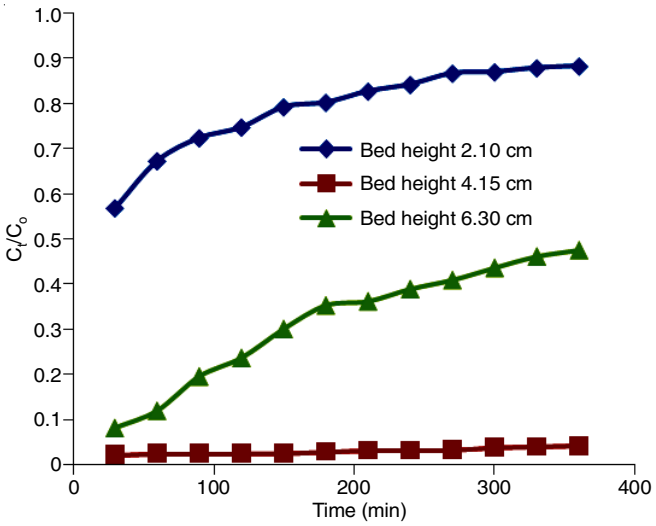

Fig. 3. Effect of bed height on the fixed-bed adsorption of metanil yellow on HNO_3- treated-H_3PO_4-activated carbon from gmelina bark

Effect of flow rate: The breakthrough curves for the adsorption of metanil yellow on gmelina bark carbon at various flow rates, influent concentration 25 mg/L and bed height 4.15 cm are shown in Fig. 4. For 6 mL/min flow rate breakthrough could not be reached within 360 min while saturation could not be reached for flow rate 17 mL/min. The equilibrium adsorption

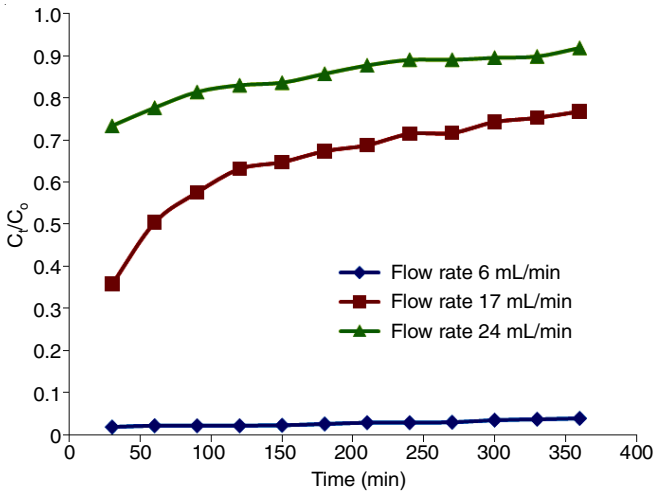

Fig. 4. Effect of flow rate on the fixed-bed adsorption of metanil yellow on HNO_3-treated-H_3PO_4-activated carbon from gmelina bark

capacities (Table-1) show that the higher the flow rate the lower the adsorption capacity. The trend is attributed to the fact that the higher the flow rate, the lower the contact time between the adsorbate and the adsorbent leading to reduction in adsorption efficiency in the bed. In addition, at higher flow rates, the movement of adsorption zone along the bed is faster reducing the time for adsorption on the adsorption on the adsorbent [12,24].

Column adsorption modelling: Thomas and Yoon-Nelson kinetic models were used to simulate the experimental data.

Thomas model: Thomas model is one of the most general and widely used methods in column performance theory. Thomas rate constant K_{Th} and adsorption capacity of the bed, q_o were determined from the plot of $\ln\{[C_o/C_t] - 1\}$ against time t (min) at various influent concentrations C_o (mg/L), bed heights and flow rates as shown in Figs. 5-7. Table-1 shows the values of K_{Th}, q_o and regression coefficients R^2. The R^2 values show that the Thomas model simulated the experimental data well. The general trend of q_o being directly proportional to C_o, q_o directly proportional to bed height and q_o inversely proportional to Q where Q is the volume flow rate was not strictly followed. Similar results were obtained by Isiuku *et al.* [1].

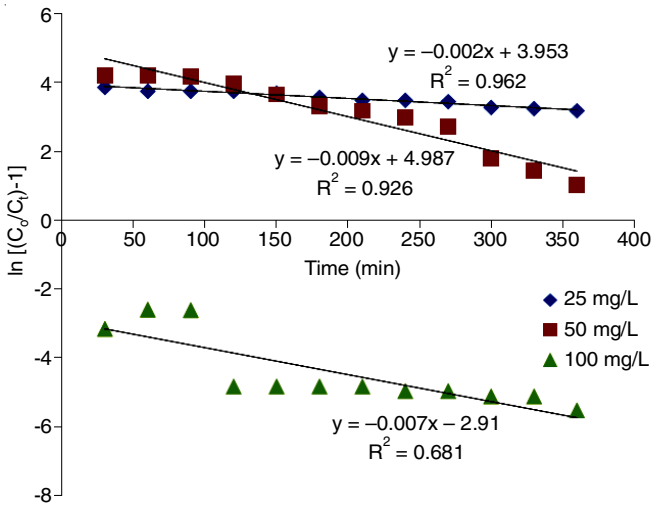

Fig. 5. Thomas model plots for the fixed-bed adsorption of metanil yellow on HNO_3-treated-H_3PO_4-activated carbon from gmelina bark at various influent concentrations

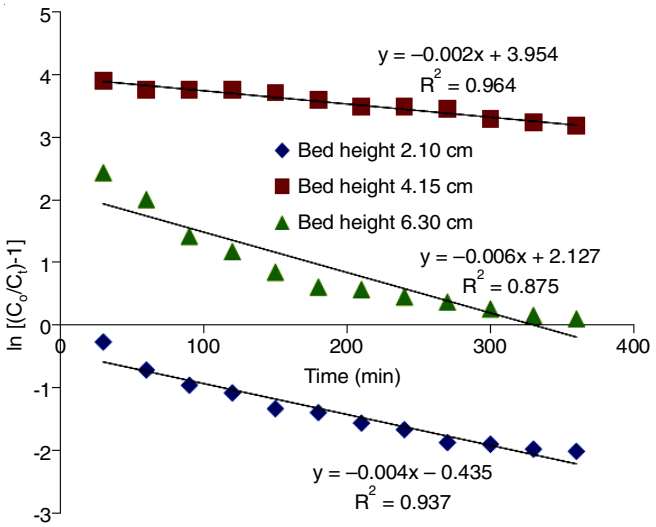

Fig. 6. Thomas model plots for the fixed –bed adsorption of metanil yellow on HNO_3-treated-H_3PO_4-activated carbon from gmelina bark at various bed heights

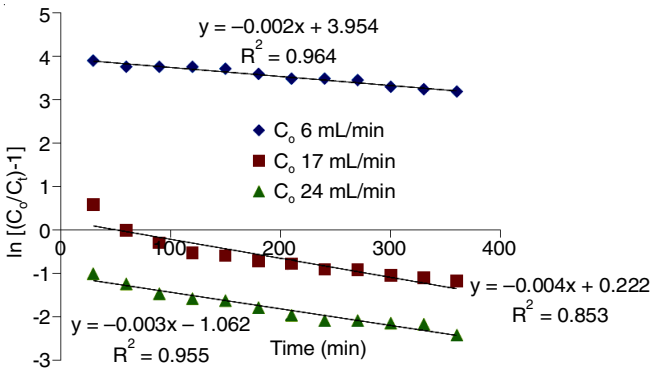

Fig. 7. Thomas model plots for the fixed-bed adsorption of metanil yellow on HNO_3-treated-H_3PO_4-activated carbon from gmelina bark at various flow rates

Yoon-Nelson model: Experimental data were simulated with the Yoon-Nelson kinetic model. Figs. 8-10 show that the $\ln [C_t/(C_o - C_t)]$ *versus* time t(min) graphs at various influent concentrations (constant bed height 4.15 cm and flow rate 6 mL/min), bed heights (constant influent concentration 25 mg/L and flow rate 6 mL/min) and flow rate (constant influent concentration 25 mg/L and bed height 4.15 cm). Table-2 shows the K_{Th}, τ, q_{oYN} and R^2 values. The experimental data exhibited good fits to the model with linear regression coefficients R^2 ranging from 0.7123 to 0.9664.

TABLE-2
THOMAS KINETIC MODEL PARAMETERS FOR THE FIXED BED ADSORPTION OF METANIL YELLOW ON GMELINA BARK CARBON

Influent conc. (mg/L)	Carbon bed height (cm)	Flow rate (mL/min)	$K_{Th} \times 10^{-5}$ (mL/min mg)	q_o (mg/g)	R^2
25	4.15	6.0	8.4	70.60	0.9627
50	4.15	6.0	19.8	37.78	0.9264
100	4.15	6.0	7.9	55.25	0.6814
25	2.10	6.0	1.96	3.33	0.9378
25	6.30	6.0	26.0	12.28	0.8758
25	4.15	17.0	14.0	31.57	0.8530
25	4.15	24.0	15.2	41.95	0.9552

TABLE-3
YOON-NELSON MODEL PARAMETERS FOR THE CARBON FIXED-BED ADSORPTION OF METANIL YELLOW ON GMELINA BARK CARBON

Influent conc. (mg/L)	Carbon bed height (cm)	Flow rate (mL/min)	K_{YN} (min^{-1})	τ (min)	q_{oYN} (mg/g)	R^2
25	4.15	6.0	0.0021	1885.1	70.69	0.9664
50	4.15	6.0	0.0098	508.46	38.14	0.9246
100	4.15	6.0	0.0089	304.69	45.70	0.7123
25	2.10	6.0	0.0049	88.78	3.33	0.9382
25	6.30	6.0	0.0065	327.62	12.29	0.8761
25	4.15	17.0	0.0044	50.64	5.38	0.8527
25	4.15	24.0	0.0038	279.82	41.97	0.9545

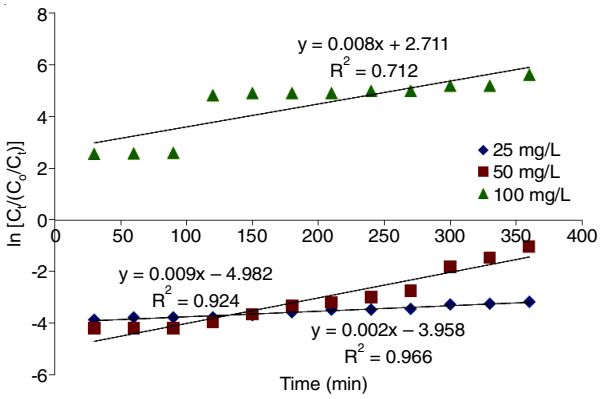

Fig. 8. Yoon-Nelson model plots for the fixed-bed adsorption of metanil yellow on HNO_3-treated-H_3PO_4-activated carbon from gmelina bark at various influent concentrations

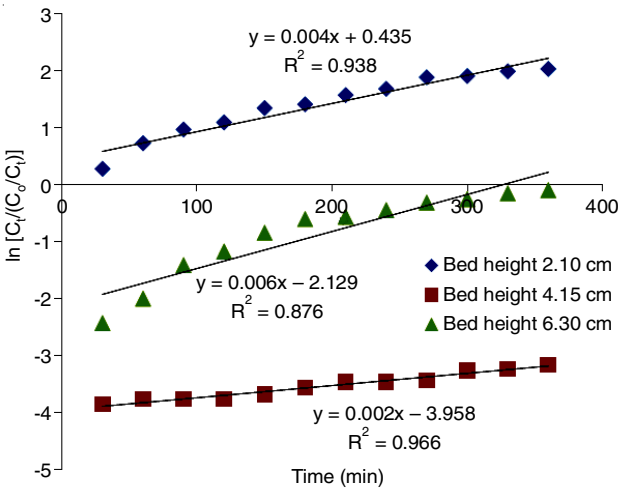

Fig. 9. Yoon-Nelson model plots for the fixed–bed adsorption of metanil yellow on HNO_3-treated-H_3PO_4-activated carbon from gmelina bark at various bed heights

Conclusion

The removal of metanil yellow from aqueous solution by adsorption on H_3PO_4-activated carbon treated with HNO_3 from gmelina bark was carried out in a fixed bed column. The parameters studied were effects of influent concentration, bed height and flow rate at 29 °C. The maximum experimental adsorption capacity 19.93 mg/g was for 50 mg/L influent concentration, 4.15 cm bed height and flow rate 6 mL/min while the highest percentage removal of 96 % was for 25 mg/L influent concentration, 4.15 cm bed height and 6 mL/min flow rate. Thomas and Yoon-Nelson kinetic models simulated experimental data well. The results show the HNO_3-treated-H_3PO_4-activated carbon from gmelina bark a good adsorbent for metanil yellow removal from aqueous solution.

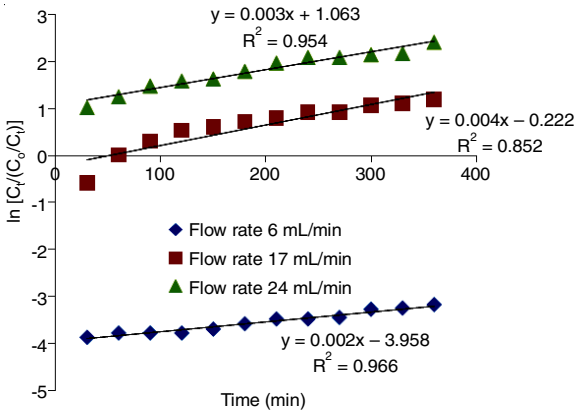

Fig. 10. Yoon-Nelson model plots for the fixed-bed adsorption of metanil yellow on HNO_3-treated H_3PO_4-activated carbon from gmelina bark at various flow rates

REFERENCES

1. O.B. Isiuku, M. Horsfall Jnr. and A.I. Spiff, *J. Eng. Appl. Sci.*, **8**, 282 (2013).
2. N. Pramanpol and N. Nittayapat, *Kasetsart J. Nat. Sci.*, **40(Suppl.)**, 192 (2006).
3. A. Mittal, V.K. Gupta, A. Malviya and J. Mittal, *J. Hazard. Mater.*, **151**, 821 (2008).
4. S. Gupta, M. Sundarrajan and K.V.K. Rao, *Tertogen. Carcin. Mut.*, **23 (Suppl. 1)**, 301 (2003).
5. R. Sivashankar, V. Sivasubramanian, A.B. Sathya and S. Pallipad, Proceedings of the International Conference on Future Trends in Structural, Civil, Environmental and Mechanical Engineering: Institute of Research Engineers and Doctors, pp. 153-157 (2013).
6. M.R.H. Mas Har and K. Sathasivam, *Am. J. Appl. Sci.*, **6**, 1690 (2009).
7. B.O. Isiuku, M. Horsfall and A.I. Spiff, *Res. J. Appl. Sci.*, **9**, 201 (2014).
8. A.A. Ahmad and B.H. Hameed, *J. Hazard. Mater.*, **175**, 298 (2010).
9. J.M. Chern and Y.N. Chien, *Water Res.*, **36**, 647 (2002).
10. B.O. Isiuku and O.U. Akakuru, *Nigerian J. Appl. Sci.*, **31**, 170 (2013).
11. J.T. Nwabanne and P.K. Igbokwe, *Int. J. Appl. Sci. Technol.*, **2**, 106 (2012).
12. H. Patel and R.T. Vashi, *Can. J. Chem. Eng.*, **90**, 180 (2012).
13. V.C. Taty-Costodes, H. Fauduet, C. Porte and Y.-S. Ho, *J. Hazard. Mater.*, **123**, 135 (2005).
14. Z. Aksu and F. Gönen, *Process Biochem.*, **39**, 599 (2004).
15. E.I. Unuabonah, B.I. Olu-Owolabi, E.I. Fasuyi and K.O. Adebowale, *J. Hazard. Mater.*, **179**, 415 (2010).
16. Y. Fu and T. Viraraghavan, *Water SA*, **29**, 465 (2003).
17. S. Kundu and A.K. Gupta, *Chem. Eng. J.*, **129**, 123 (2007).
18. P. Sivakumar and P.N. Palanisamy, *J. Chem. Technol. Rev.*, **1**, 502 (2009).
19. K. Baek, S. Song, S. Kang, Y. Rhee, C. Lee, B. Lee, S. Hudson and T. Hwang, *J. Ind. Eng. Chem.*, **13**, 452 (2007).
20. U. Thawornchaisit and K. Pakulanon, *Bioresour. Technol.*, **98**, 140 (2007).
21. Z. Aksu and D. Akpinar, *Sep. Purif. Technol.*, **21**, 87 (2000).
22. Z. Aksu and J. Yener, *Waste Manage.*, **21**, 695 (2001).
23. J.M. Salman, V.O. Njoku and B.H. Hameed, *Chem. Eng. J.*, **174**, 33 (2011).
24. O. Ozdemir, M. Turan, A.Z. Turan, A. Faki and A.B. Engin, *J. Hazard. Mater.*, **166**, 647 (2009).